Influence of Na^+ on the Stoichiometry of Carbonated Hydroxyapatite Obtained by the Hydrolysis of Octacalcium Phosphate

Ilse Y. Pieters,[†] Erna A. P. De Maeyer,[‡,§] and Ronald M. H. Verbeeck*[,‡]

Laboratory for Analytical Chemistry and Department of Dental Materials Science, Institute for Biomedical Technologies (IBITECH), University Hospital, University of Ghent, De Pintelaan 185 (P8) B-9000 GHENT, Belgium

Received March 12, 1998

Introduction

Calcium hydroxyapatite (HAp), $Ca_{10}(PO_4)_6(OH)_2$, is generally considered as the prototype for the inorganic compound of calcifications in higher vertebrates. However, these apatites also contain some sodium and carbonate, which affect the (de)-mineralization processes of these biominerals.[1] It is then not surprising that numerous investigators tried to deduce the mechanisms for carbonate incorporation (for a survey see ref 2).

According to De Maeyer,[3] every mechanism for CO_3^{2-} and/or alkali metal incorporation proposed in the literature can be related to six basic substitution mechanisms:

$$Ca^{2+} + PO_4^{3-} + OH^- \leftrightarrow V^{Ca} + CO_3^{2-} + V^{OH} \quad \text{(I)}$$

$$Ca^{2+} + 2PO_4^{3-} \leftrightarrow V^{Ca} + 2CO_3^{2-} \quad \text{(II)}$$

$$Ca^{2+} + PO_4^{3-} \leftrightarrow M^+ + CO_3^{2-} \quad \text{(III)}$$

$$Ca^{2+} + OH^- \leftrightarrow M^+ + V^{OH} \quad \text{(IV)}$$

$$PO_4^{3-} \leftrightarrow CO_3^{2-} + OH^- \quad \text{(V)}$$

$$2OH^- \leftrightarrow CO_3^{2-} + V^{OH} \quad \text{(VI)}$$

with V^X a vacancy on an apatite lattice site occupied by X and M an alkali metal.

In a previous study, it was shown that the stoichiometry of K^+- and CO_3^{2-}-containing apatites (KCAp's) obtained by the hydrolysis of octacalcium phosphate (OCP), $Ca_8(HPO_4)_2(PO_4)_4 \cdot 5H_2O$, is mainly determined by the substitution mechanisms I and III.[4] The same holds for the stoichiometry of CO_3^{2-}- and Na^+- or K^+-containing apatites prepared by the hydrolysis of monetite ($CaHPO_4$).[2,5] However, both the nature of the alkali metal and the starting reagent (OCP or monetite) strongly determine the absolute and relative contribution of the occurring mechanisms. To further corroborate these findings, the present study investigates the stoichiometry of Na^+- and CO_3^{2-}-containing apatites (NCAp's) prepared by the hydrolysis of OCP in Na^+- and CO_3^{2-}-containing solutions. These synthetic samples also have biological importance, because OCP is thought to be an essential precursor in the formation of biological apatites.[6−8]

Experimental Section

The materials and methods are described in detail in ref 4, except for the items mentioned below.

NCAp's were prepared using Na_2CO_3 and $NaNO_3$ (Merck, Pro Analysi) as reagents. The carbonate concentration in the solution c_{nc} ranged from 0.0025 to 0.05 M and the hydrolysis time was 24 h.

The sodium content of the precipitates was determined with a Varian SpectrAA-30 atomic absorption spectrophotometer.

Results

Chemical Composition. Table 1 summarizes the chemical composition of the precipitates. %OH and Σ% were calculated from the analysis data as outlined in our previous study.[4] The errors on $\%HPO_4$, %OH, and %Σ were estimated by error propagation theory (95% confidence level).

Table 1 shows that the Ca, PO_4, and OH contents of the solid decrease with increasing c_{nc}. The Ca content also tends to decrease with increasing R at a given c_{nc}. This also applies for the OH content for values of $c_{nc} > 0.005$ M. The PO_4 content is independent of R within the experimental error. The CO_3 content as well as the Na content of the precipitates increase with increasing c_{nc} and R. The HPO_4 content tends to increase with increasing c_{nc} and decreases with increasing R at a given c_{nc}. The total mass balance (%Σ) is significantly lower than 100% and decreases with increasing CO_3 content, indicating that the samples still contain 3.5−5% water, which is comparable with the results found for the KCAp's.[4]

Physical Analysis. The X-ray diffraction patterns of the samples are typical for the hexagonal lattice structure of HAp.[9] As for the KCAp's,[4] the resolution of the diffraction peaks decreases and their relative intensities change with increasing c_{nc}.

In Figure 1 the full widths at half-maximum (fwhm) of the [002] and [300] diffraction peaks are given as a function of the carbonate content of the precipitates. The fwhm is indicative for the effect of c_{nc} and R on the crystallinity of the samples (crystal size and/or lattice perfection).[4,10−12] The width of the [300] diffraction peak increases with increasing carbonate

* To whom correspondence and reprint requests should be adressed.
[†] Laboratory for Analytical Chemistry.
[‡] Department of Dental Materials Science.
[§] Senior Research Assistant of the FSR-Flanders (Belgium).

(1) Driessens, F. C. M.; Verbeeck, R. M. H. *Biominerals*; CRC Press: Boca Raton, FL, 1990.
(2) De Maeyer, E. A. P.; Verbeeck, R. M. H.; Naessens, D. E. *Inorg. Chem.* **1993**, *32*, 5709−5714.
(3) De Maeyer, E. A. P.; Verbeeck, R. M. H. *Bull. Soc. Chem. Belg.* **1993**, *102*, 601−609.
(4) Pieters, I. Y.; De Maeyer, E. A. P.; Verbeeck, R. M. H. *Inorg. Chem.* **1996**, *35*, 5791−5797.
(5) De Maeyer, E. A. P.; Verbeeck, R. M. H.; Pieters, I. Y. *Inorg. Chem.* **1996**, *35*, 857−863.
(6) Brown, W. E.; Smith, J. P.; Lehr, J. R.; Frazier A. W. *Nature* **1962**, *196*, 1050−1055.
(7) Weiss, M. P.; Voegel, J. C.; Frank, R. M. *J. Ultrastruct. Res.* **1981**, *76*, 286−292.
(8) Bodier-Houllé, P.; Steuer, P., Voegel, J. C.; Cuisinier, F. J. G. *J. Dent. Res.* **1998**, *77*, 917 (abstract #2287).
(9) ASTM-Powder Diffraction Data File #9-432.
(10) LeGeros, R. Z.; LeGeros, J. P.; Trautz, O. R.; Shirra, W. P. *Adv. X-ray Anal.* **1971**, *14*, 57−66.
(11) LeGeros, R. Z.; Trautz, O. R.; LeGeros, J. P.; Klein, E.; Shirra, W. P. *Science* **1967**, *155*, 1409−1411.
(12) Doi, Y.; Moriwaki, Y.; Aoba, T.; Takahashi, J.; Joshin, K. *Calcif. Tissue Int.* **1982**, *34*, 178−181.

10.1021/ic9802810 CCC: $15.00 © 1998 American Chemical Society
Published on Web 11/04/1998

Table 1. Chemical Composition (Weight Percent)[a] and Total Mass Balance (%Σ) of the Precipitates Dried at 25 °C to Constant Weight as a Function of the Na_2CO_3 Concentration (c_{nc}) and the Molar Na/CO_3 Ratio (R) of the Hydrolysis Solution

sample	c_{nc} (M)	R	%Ca	%PO_4	%HPO_4	%CO_3	%Na	%OH	%Σ
H2a	0.0025	2	37.23	50.90	2.23 ± 0.30	2.87	0.56	2.25 ± 0.11	96.04 ± 0.16
H2b		2	37.35	50.93	2.48 ± 0.30	2.85	0.57	2.26 ± 0.11	96.44 ± 0.16
H5		5	37.21	50.84	2.26 ± 0.30	2.99	0.71	2.30 ± 0.11	96.31 ± 0.16
H10a		10	37.10	50.81	2.05 ± 0.29	3.24	0.83	2.24 ± 0.11	96.26 ± 0.16
H10b		10	37.17	50.53	2.63 ± 0.30	3.25	0.85	2.25 ± 0.11	96.69 ± 0.16
H15		15	37.04	50.50	2.42 ± 0.29	3.33	0.92	2.24 ± 0.11	96.45 ± 0.16
H20		20	36.86	50.68	1.89 ± 0.29	3.45	0.95	2.13 ± 0.11	95.96 ± 0.16
I2	0.0050	2	36.93	49.67	2.76 ± 0.29	3.63	0.84	2.24 ± 0.11	96.07 ± 0.16
I5		5	36.92	49.67	2.51 ± 0.29	4.00	1.00	2.23 ± 0.11	96.33 ± 0.16
I10		10	36.79	49.79	2.17 ± 0.29	4.26	1.11	2.11 ± 0.11	96.23 ± 0.16
I15		15	36.65	49.49	2.20 ± 0.29	4.52	1.20	2.06 ± 0.11	96.12 ± 0.16
I20a		20	36.63	49.83	1.92 ± 0.29	4.65	1.36	2.01 ± 0.12	96.40 ± 0.17
I20b		20	36.58	49.49	1.92 ± 0.29	4.70	1.33	2.10 ± 0.12	96.12 ± 0.17
J2a	0.010	2	36.48	48.45	2.97 ± 0.29	4.51	1.07	2.11 ± 0.11	95.59 ± 0.16
J2b		2	36.57	48.75	3.16 ± 0.29	4.54	1.11	1.97 ± 0.12	96.11 ± 0.16
J5		5	36.53	48.78	2.32 ± 0.28	5.00	1.26	2.07 ± 0.12	95.96 ± 0.16
J10		10	36.33	48.60	2.14 ± 0.28	5.54	1.51	1.95 ± 0.12	96.06 ± 0.16
J15a		15	36.24	48.69	1.92 ± 0.28	5.75	1.59	1.83 ± 0.12	96.02 ± 0.17
J15b		15	36.20	48.54	1.95 ± 0.28	5.89	1.60	1.80 ± 0.12	95.98 ± 0.17
J20		20	36.18	48.54	1.80 ± 0.28	5.88	1.55	1.81 ± 0.12	95.75 ± 0.17
K2	0.025	2	36.08	47.92	2.63 ± 0.28	6.17	1.57	1.60 ± 0.12	95.98 ± 0.17
K5		5	35.97	47.43	2.42 ± 0.28	6.52	1.69	1.74 ± 0.12	95.77 ± 0.17
K10		10	35.69	47.59	1.74 ± 0.27	6.89	2.01	1.69 ± 0.13	95.60 ± 0.18
K15		15	35.58	47.50	1.67 ± 0.27	7.29	2.05	1.47 ± 0.13	95.56 ± 0.18
L2a	0.050	2	35.59	46.85	2.97 ± 0.28	6.38	1.74	1.65 ± 0.12	95.19 ± 0.17
L2b		2	35.58	46.94	2.97 ± 0.28	6.40	1.84	1.66 ± 0.12	95.39 ± 0.17
L5		5	35.50	46.85	2.14 ± 0.27	7.45	2.07	1.51 ± 0.13	95.52 ± 0.18
L10a		10	35.13	46.33	1.98 ± 0.27	8.09	2.21	1.27 ± 0.13	95.01 ± 0.18
L10b		10	35.13	46.48	1.89 ± 0.27	8.21	2.37	1.27 ± 0.13	95.35 ± 0.18

[a] The relative uncertainties on the amount of Ca, PO_4, Na, and CO_3 were determined as 0.2, 0.6, 2, and 2%, respectively.

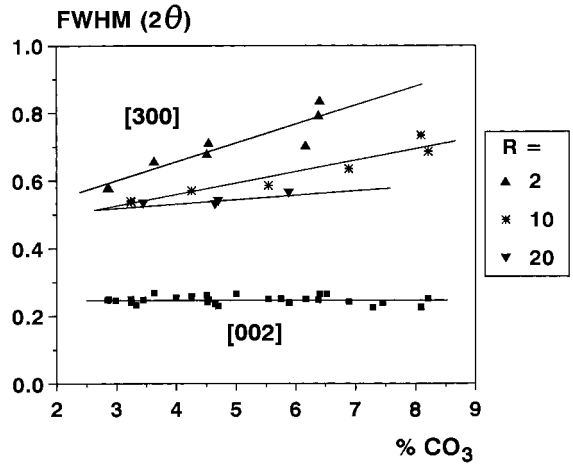

Figure 1. Full width at half-maximum (fwhm) of the [002] and [300] diffraction peak as a function of the carbonate content (wt %) at a given molar Na/CO_3 ratio R in the hydrolysis solution.

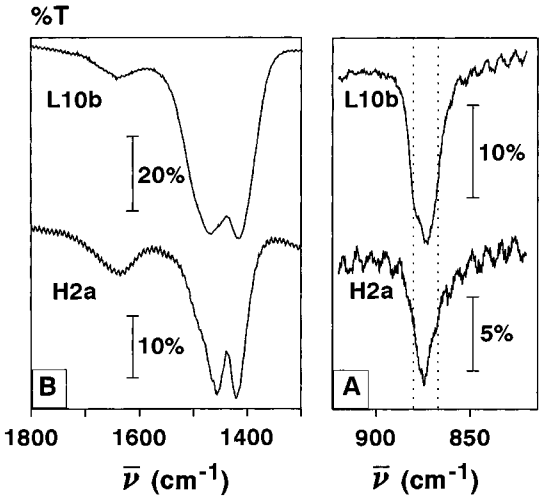

Figure 2. IR spectra of samples H2a and L10b in the carbonate absorption region between 820 and 920 cm^{-1} (A) and between 1300 and 1800 cm^{-1} (B) (% transmittance versus wavenumber).

content of the solid, but decreases with increasing R values in the hydrolysis solution. The width of the [002] reflection remains constant within the experimental error. This indicates that the crystallinity of the NCAp's in the a direction of the hexagonal lattice is influenced by the incorporation of CO_3^{2-} and alkali metal, whereas the crystallinity along the c axis is obviously not affected, sustaining the findings of other studies.[4,13,14] However, LeGeros[10,11] found the opposite effect for carbonated apatites obtained by the hydrolysis of monetite.

A weighted regression analysis shows that the a axis parameter as well as the c axis parameter are independent of R but decrease and increase respectively with increasing CO_3 content of the solid according to:

$$a\ (\text{nm}) = (0.9423 \pm 0.0008) - (5.9 \pm 1.6) \times 10^{-4}\,[\%CO_3] \quad (1)$$

$$c\ (\text{nm}) = (0.6879 \pm 0.0004) + (1.9 \pm 0.7) \times 10^{-4}\,[\%CO_3] \quad (2)$$

The IR absorptions of PO_4^{3-}, OH^-, and H_2O of the NCAp's are comparable to the respective absorptions of the KCAp's.[4] Figure 2A and B gives the CO_3^{2-} absorptions of two representative samples in the regions 820−920 cm^{-1} (bending mode) and

(13) Chickerur, N. S.; Tung, M. S.; Brown, W. E. *Calcif. Tissue Int.* **1980**, *32*, 55−62.
(14) Trautz, O. R. *Ann. N.Y. Acad. Sci.* **1960**, *85*, 145−160.

Table 2. Unit Cell Content of the Precipitates Calculated from the Data in Table 1

sample	n_{Ca}	n_{PO_4}	n_{CO_3}	n_{Na}	n_{HPO_4}	n_{OH}	n_V^{Ca}	n_V^{OH}
H2a	9.181 ± 0.029	5.298 ± 0.029	0.473 ± 0.009	0.241 ± 0.005	0.230 ± 0.030	1.306 ± 0.072	0.348 ± 0.042	0.464 ± 0.067
H2b	9.172 ± 0.029	5.278 ± 0.029	0.467 ± 0.009	0.244 ± 0.005	0.254 ± 0.030	1.310 ± 0.072	0.330 ± 0.042	0.436 ± 0.067
H5	9.152 ± 0.029	5.276 ± 0.029	0.491 ± 0.009	0.304 ± 0.006	0.232 ± 0.030	1.331 ± 0.073	0.312 ± 0.042	0.437 ± 0.067
H10a	9.100 ± 0.029	5.259 ± 0.029	0.531 ± 0.010	0.355 ± 0.007	0.210 ± 0.030	1.297 ± 0.075	0.335 ± 0.043	0.493 ± 0.067
H10b	9.068 ± 0.029	5.203 ± 0.029	0.530 ± 0.010	0.362 ± 0.007	0.268 ± 0.030	1.294 ± 0.075	0.302 ± 0.043	0.438 ± 0.068
H15	9.054 ± 0.029	5.209 ± 0.029	0.544 ± 0.010	0.392 ± 0.008	0.247 ± 0.030	1.290 ± 0.075	0.307 ± 0.043	0.463 ± 0.067
H20	9.033 ± 0.030	5.242 ± 0.029	0.565 ± 0.010	0.406 ± 0.008	0.193 ± 0.030	1.229 ± 0.077	0.368 ± 0.043	0.578 ± 0.067
I2	9.029 ± 0.030	5.125 ± 0.029	0.593 ± 0.011	0.358 ± 0.007	0.282 ± 0.030	1.292 ± 0.078	0.331 ± 0.043	0.426 ± 0.068
I5	8.975 ± 0.031	5.096 ± 0.029	0.649 ± 0.012	0.424 ± 0.009	0.255 ± 0.029	1.277 ± 0.080	0.346 ± 0.044	0.468 ± 0.068
I10	8.913 ± 0.031	5.091 ± 0.029	0.689 ± 0.012	0.469 ± 0.009	0.220 ± 0.029	1.204 ± 0.082	0.398 ± 0.044	0.576 ± 0.069
I15	8.859 ± 0.032	5.048 ± 0.029	0.730 ± 0.013	0.506 ± 0.010	0.222 ± 0.029	1.175 ± 0.085	0.413 ± 0.044	0.603 ± 0.069
I20a	8.814 ± 0.032	5.060 ± 0.029	0.747 ± 0.013	0.571 ± 0.012	0.193 ± 0.029	1.139 ± 0.086	0.422 ± 0.045	0.668 ± 0.069
I20b	8.841 ± 0.032	5.047 ± 0.029	0.759 ± 0.013	0.560 ± 0.011	0.194 ± 0.029	1.194 ± 0.086	0.405 ± 0.045	0.612 ± 0.070
J2a	8.862 ± 0.032	4.967 ± 0.029	0.732 ± 0.013	0.453 ± 0.009	0.301 ± 0.029	1.209 ± 0.084	0.384 ± 0.044	0.490 ± 0.069
J2b	8.803 ± 0.031	4.952 ± 0.029	0.730 ± 0.013	0.466 ± 0.009	0.318 ± 0.029	1.119 ± 0.084	0.413 ± 0.044	0.563 ± 0.069
J5	8.804 ± 0.033	4.962 ± 0.029	0.805 ± 0.014	0.529 ± 0.011	0.233 ± 0.029	1.173 ± 0.088	0.434 ± 0.045	0.594 ± 0.070
J10	8.683 ± 0.034	4.902 ± 0.030	0.884 ± 0.015	0.629 ± 0.013	0.214 ± 0.028	1.096 ± 0.093	0.474 ± 0.046	0.690 ± 0.071
J15a	8.632 ± 0.035	4.894 ± 0.030	0.915 ± 0.016	0.660 ± 0.013	0.191 ± 0.028	1.028 ± 0.094	0.517 ± 0.047	0.781 ± 0.071
J15b	8.608 ± 0.035	4.871 ± 0.030	0.935 ± 0.016	0.663 ± 0.013	0.194 ± 0.028	1.008 ± 0.095	0.535 ± 0.047	0.798 ± 0.072
J20	8.627 ± 0.035	4.884 ± 0.030	0.936 ± 0.016	0.664 ± 0.013	0.179 ± 0.028	1.015 ± 0.095	0.530 ± 0.047	0.806 ± 0.072
K2	8.508 ± 0.035	4.769 ± 0.030	0.972 ± 0.016	0.645 ± 0.013	0.259 ± 0.028	0.890 ± 0.097	0.588 ± 0.047	0.851 ± 0.072
K5	8.502 ± 0.037	4.732 ± 0.030	1.029 ± 0.017	0.696 ± 0.014	0.239 ± 0.027	0.970 ± 0.100	0.563 ± 0.048	0.791 ± 0.074
K10	8.427 ± 0.038	4.742 ± 0.030	1.087 ± 0.018	0.827 ± 0.017	0.172 ± 0.027	0.941 ± 0.103	0.574 ± 0.049	0.887 ± 0.075
K15	8.336 ± 0.038	4.696 ± 0.030	1.141 ± 0.019	0.837 ± 0.017	0.163 ± 0.027	0.812 ± 0.106	0.664 ± 0.050	1.025 ± 0.075
L2a	8.449 ± 0.036	4.694 ± 0.030	1.011 ± 0.017	0.720 ± 0.015	0.294 ± 0.027	0.923 ± 0.099	0.537 ± 0.048	0.783 ± 0.073
L2b	8.429 ± 0.036	4.693 ± 0.030	1.013 ± 0.017	0.760 ± 0.015	0.294 ± 0.027	0.924 ± 0.099	0.517 ± 0.048	0.782 ± 0.073
L5	8.307 ± 0.039	4.627 ± 0.031	1.164 ± 0.019	0.844 ± 0.017	0.209 ± 0.027	0.833 ± 0.109	0.640 ± 0.051	0.958 ± 0.076
L10a	8.175 ± 0.040	4.550 ± 0.031	1.257 ± 0.020	0.897 ± 0.018	0.192 ± 0.026	0.698 ± 0.112	0.736 ± 0.051	1.110 ± 0.078
L10b	8.141 ± 0.040	4.546 ± 0.031	1.271 ± 0.020	0.958 ± 0.020	0.183 ± 0.026	0.693 ± 0.113	0.718 ± 0.052	1.124 ± 0.078

1400−1600 cm^{-1} (stretching mode), respectively. In Figure 2A, the peak maximum of the CO_3^{2-} band is situated near 874 cm^{-1}, which is typical for B-type CO_3^{2-} (i.e CO_3^{2-} substituting on a PO_4^{3-} lattice site).[1] An asymmetry of the peak near 865 cm^{-1} arises from vibrations of the HPO_4^{2-} ions.[15] For the higher carbonated NCAp's (e.g. sample L10b), a weak shoulder near 880 cm^{-1} could be attributed to the A-type CO_3^{2-} bending mode (i.e. CO_3^{2-} substituting on an OH^- lattice site).[16,17] Figure 2B shows that the major absorptions of the CO_3^{2-} stretching mode are situated near 1420 and 1455 cm^{-1} typical for B-type CO_3^{2-}.[1] However, some shoulders can be observed at higher wavenumbers ($1470 \leq \nu\ (cm^{-1}) \leq 1550$), possibly indicative for A-type CO_3^{2-}.[18,19]

Discussion

As for the KCAp's,[4] the presence of HPO_4^{2-}, originating from unreacted OCP layers in the crystallites, is related to the carbonate content and to the broadening of the [300] reflection with increasing c_{nc}, suggesting the inhibition of the transformation of OCP to apatite by carbonate.[4,13] The decrease of the broadening of the [300] reflection with increasing R (Figure 1) was not observed for the KCAp's[6] and is related to the decrease of the HPO_4^{2-} content of the NCAp's as a function of R (Table 1). An increase of the molar Na/CO_3 ratio R in the hydrolysis solution seems to partially compensate the inhibitory effect of carbonate.

The contraction of the a axis and the slight expansion of the c axis with increasing carbonate content of the samples (eqs 1 and 2) agree with the results of De Maeyer et al.[2] and LeGeros et al.[10] indicating the occurrence of B-type CO_3^{2-} in the apatite lattice.[1] This was to be expected, in view of the results for the analogously synthesized KCAp's.[4] As discussed in our previous studies,[5,20] the weak IR absorptions near 880 cm^{-1} and between 1470 and 1550 cm^{-1} are to be ascribed to different environments of the B-type CO_3^{2-} ions in the apatite lattice and not to an A-type CO_3^{2-} -incorporation.

To deduce the mechanisms for Na^+- and B-type CO_3^{2-} -incorporation in HAp, the absolute content of the unit cell of the NCAp's must be known. The presence of water makes it impossible to deduce the absolute content of the unit cell.[4] However, the fact that no A-type CO_3^{2-} is present in these samples implies that mechanism VI does not contribute so that the following equation holds:

$$n_p + n_{CO_3} = 6 \tag{3}$$

with

$$n_p = n_{PO_4} + n_{HPO_4} \tag{4}$$

where n_X represents the number of X ions per unit cell.

On the basis of eq 3 and the chemical composition of the samples, the mean content of the unit cell of the apatites can be calculated as outlined before.[4] The results of this calculation are given in Table 2. From the independent parameters n_{Ca}, n_{PO_4}, and n_{Na}, the values of n_{OH}, n_{CO_3} and n_{HPO_4} can be calculated on the basis of electroneutrality and eqs 3 and 4, respectively. The number of vacancies on Ca^{2+} and OH^- lattice sites in the apatite cell, respectively given by eqs 5 and 6 are also given in Table 2. The errors in Table 2 were estimated by error propagation theory.

(15) Berry, E. E. *J. Inorg. Nucl. Chem.* **1967**, *29*, 317−327.
(16) Bonel, G. *Ann. Chim.* **1972**, *7*, 65−88 and 127−144.
(17) Rey, C.; Collins, B.; Goehl, T.; Dickson, I. R.; Glimcher, M. J. *Calcif. Tissue Int.* **1989**, *45*, 157−164.
(18) Vignoles, M.; Bonel, G.; Holcomb, D. W.; Young, R. A. *Calcif. Tissue Int.* **1988**, *43*, 33−40.
(19) LeGeros, R. Z.; Abergas, T.; Bleiwas, H.; LeGeros, J. P. *J. Dent. Res.* **1987**, *66*, 190 (abstract #667).
(20) De Maeyer, E. A. P.; Verbeeck, R. M. H.; Naessens, D. E. *Inorg. Chem.* **1994**, *33*, 5999−6006.

$$n_{VCa} = 10 - n_{Ca} - n_{Na} - n_{HPO_4} \quad (5)$$

$$n_{VOH} = 2 - n_{OH} - n_{HPO_4} \quad (6)$$

From Table 2, it can be seen that for every sample

$$n_{VOH} > n_{Na} \quad (7)$$

which can only be accounted for by the individual B-type CO_3^{2-} -incorporation according to mechanism I. The occurrence of this mechanism is corroborated by the fact that, according to Table 1, the OH^- content of the solid decreases with increasing c_{nc} at a given R and hence with an increasing CO_3 content of the solid. Moreover,

$$n_{VCa} < n_{VOH} \quad (8)$$

indicating that mechanism IV (individual Na^+-incorporation), which creates vacancies on the OH^- lattices sites, contributes to the global stoichiometry as well. If only mechanisms I and IV would contribute, however, eq 9 would hold, which is not the case (Table 2).

$$n_{VOH} - n_{VCa} = n_{Na} \quad (9)$$

In this respect, mechanisms II, III, and V should be considered as well. Mechanism II was only found to contribute to a small extent in KCAp's prepared by the hydrolysis of monetite[5] or by heterogeneous precipitation.[21] Mechanism V represents a coupled CO_3^{2-} -OH^- substitution for PO_4^{3-} and is expected to lead to characteristic absorptions in the IR spectra due to strong interactions between the negatively charged CO_3^{2-} and OH^- ions on the same lattice site. As such effect is not observed, the occurrence of mechanism V is improbable. Moreover, the positive correlation between n_{Na} and n_{CO_3} (Table 2) suggests the occurrence of a coupled $Na^+-CO_3^{2-}$ incorporation according to mechanism III.

On this basis it can be concluded that most probably mechanisms I, III and IV determine the composition of the NCAp's prepared in this study. The mean stoichiometry of the interlayered mixtures of OCP and carbonated apatite can then be represented by formula (10)

$$Ca_{10-x-y-z-u}Na_{y+z}(PO_4)_{6-x-y-u}(HPO_4)_u(CO_3)_{x+y}(OH)_{2-x-z-u} \quad (10)$$

where

$$u = n_{HPO_4} \quad (11)$$

and x, y, and z, respectively, are the contributions per unit cell of the mechanisms I, III, and IV, given by

$$x = n_{VCa} \quad (12)$$

$$y = n_{CO_3} - x \quad (13)$$

$$z = n_{Na} - y \quad (14)$$

Figure 3 represents the contributions of x, y, and z as a function of n_{CO_3} for the different values of c_{nc}. This figure shows that no constant ratio exists between these contributions, corroborating that these mechanisms can occur independently.[2,4,5,20] For $c_{nc} < 0.025$ M, the contribution z of the individual Na^+-incorporation (mechanism IV) apparently is independent of c_{nc} but increases from 0.1 to 0.25 with increasing R (Figure 3B). For $c_{nc} \geq 0.025$ M, z increases and varies between 0.25 and 0.40 with R at a given c_{nc}. x and y tend to increase as well with increasing R, although the relative increase is smaller and not always significant. Hence, an increase of the Na^+ concentration in the solution mainly stimulates the individual Na^+ incorporation (z). This is in line with the results obtained for NCAp's prepared by the hydrolysis of monetite.[22] The decrease of the [300] diffraction peak with increasing R (Figure 1) could then indicate that mechanism IV compensates the inhibitory effect of carbonate on the hydrolysis of OCP and hence promotes its conversion to apatite. From Figure 3, it can further be seen that x and z start to increase when y reaches its maximum value. A competition between mechanisms I and IV on one hand and III on the other hand seems to turn out in favor of mechanism III at low c_{nc} values.

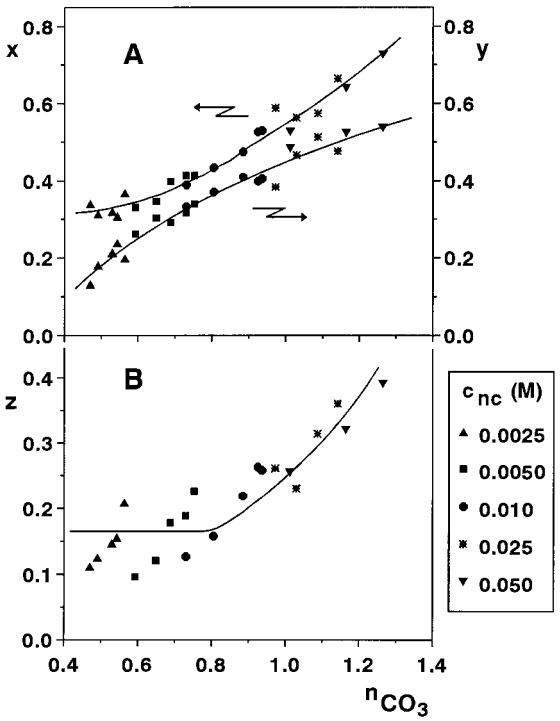

Figure 3. Contribution x and y per unit cell of mechanisms I and III (A) and contribution z of mechanism IV (B) to the stoichiometry of the NCAp's as a function of the number of carbonate ions per unit cell (n_{CO_3}) at different c_{nc}.

Conclusions

The type of mechanisms found in the present study are well in line with the results obtained for NCAp's prepared by the hydrolysis of $CaHPO_4$,[20] although their contributions per unit cell as a function of c_{nc} differ significantly.[21] This indicates that, apart from the solution characteristics, the specific crystallization kinetics drastically affect the precipitates stoichiometry. This should be taken into account when using the results of synthetic apatites to explain or predict biomineralization.

Acknowledgment. This work is part of a project supported by the "Excecutieve van de Vlaamse Gemeenschap—Departement Onderwijs," which is gratefully acknowledged.

IC9802810

(21) De Maeyer, E. A. P.; Verbeeck, R. M. H.; Pieters, I. Y. *Trends in Inorg. Chem.* **1996**, *4*, 157−171.

(22) De Maeyer, E. A. P.; Verbeeck, R. M. H.; Pieters, I. Y. *J. Crystal Growth* **1996**, *169*, 539−547.